Development 135, 1147-1156 (2008) doi:10.1242/dev.018150

The ATPase-dependent chaperoning activity of Hsp90a regulates thick filament formation and integration during skeletal muscle myofibrillogenesis

Thomas A. Hawkins[1], Anna-Pavlina Haramis[1,*], Christelle Etard[2], Chrisostomos Prodromou[3], Cara K. Vaughan[3], Rachel Ashworth[4,†], Saikat Ray[1], Martine Behra[2,‡], Nigel Holder[1], William S. Talbot[5], Laurence H. Pearl[3], Uwe Strähle[2] and Stephen W. Wilson[1,§]

The mechanisms that regulate sarcomere assembly during myofibril formation are poorly understood. In this study, we characterise the zebrafish *sloth*^{u45} mutant, in which the initial steps in sarcomere assembly take place, but thick filaments are absent and filamentous I-Z-I brushes fail to align or adopt correct spacing. The mutation only affects skeletal muscle and mutant embryos show no other obvious phenotypes. Surprisingly, we find that the phenotype is due to mutation in one copy of a tandemly duplicated *hsp90a* gene. The mutation disrupts the chaperoning function of Hsp90a through interference with ATPase activity. Despite being located only 2 kb from *hsp90a*, *hsp90a2* has no obvious role in sarcomere assembly. Loss of Hsp90a function leads to the downregulation of genes encoding sarcomeric proteins and upregulation of *hsp90a* and several other genes encoding proteins that may act with Hsp90a during sarcomere assembly. Our studies reveal a surprisingly specific developmental role for a single Hsp90 gene in a regulatory pathway controlling late steps in sarcomere assembly.

KEY WORDS: Chaperones, Myofibrillogenesis, Zebrafish

INTRODUCTION

Myofibrils are the subcellular contractile apparatus of cardiac and striated muscle cells. Within each myofibril, Actin, Myosin and many other proteins are organised into reiterative arrays of sarcomeres. We understand how the intra- and extra-sarcomeric components of muscles fit together (Clark et al., 2002; Sellers, 2004), how muscle fibres are triggered to contract and how the sarcomere transduces force (Cooke, 2004; Rossi and Dirksen, 2006). However, despite this depth of knowledge of the structure and biophysics of the sarcomere and its constituents, our grasp of myofibrillogenesis, the process by which it takes form, remains surprisingly obscure.

During myofibrillogenesis, the first true sarcomeric components to appear are Actin filaments (Ehler et al., 1999; Van der Ven et al., 1999), which assemble into I-Z-I bodies/brushes, structures consisting of Z-discs flanked on both sides by Actin filaments (Schultheiss et al., 1990). The giant sarcomeric protein Titin integrates onto the nascent sarcomere around the stage that Z-disc and I-band epitopes are first present (Fürst et al., 1989). It is thought that thick filaments are subsequently assembled onto this scaffold.

[1]Department of Anatomy and Developmental Biology, UCL, Gower Street, London WC1E 6BT, UK. [2]Institute of Toxicology and Genetics, Forschungszentrum Karlsruhe, Postfach 3640, Karlsruhe, D-76021, Germany. [3]Section of Structural Biology, The Institute of Cancer Research, Chester Beatty Laboratories, 237 Fulham Road, London, SW3 6JB, UK. [4]Department of Physiology, UCL, Gower Street, London WC1E 6BT, UK. [5]Department of Developmental Biology, Stanford University School of Medicine, Beckman Center B315, 279 Campus Drive, Stanford, CA 94305-5329, USA.

*Present address: Netherlands Cancer Institute (NKI), Department of Molecular Genetics, Plesmanlaan 121, 1066 CX Amsterdam, The Netherlands
†Present address: School of Biological and Chemical Sciences, Queen Mary University of London, London E1 4NS, UK
‡Present address: National Human Genome Research Center, National Institutes of Health, Building 50, Room 5537, 50 South Drive, Bethesda, MD 20892-8004, USA
§Author for correspondence (e-mail: s.wilson@ucl.ac.uk)

Accepted 10 January 2008

The mechanisms by which thick filaments incorporate are controversial and three models have emerged. The first proposes that thick filaments form independently from I-Z-I brushes and these two separate sarcomeric components are integrated to form striated myofibrils (Holtzer et al., 1997; Schultheiss et al., 1990). The second holds that pre-myofibrils are first constructed from non-muscle Myosin, which is later replaced by muscle Myosin to form functional sarcomeres (LoRusso et al., 1997; Rhee et al., 1994; Sanger et al., 2002). The third theory proposes that Titin is a scaffold upon which other sarcomeric components are assembled (Ehler et al., 1999; Gregorio et al., 1999; Trinick and Tskhovrebova, 1999; Van der Ven et al., 1999). The idea is that the N-terminal portion of Titin first associates with the Z-disc and I-band (forming I-Z-I brushes). These complexes are then brought into register, either by the unfolding of the Titin filament or further translation, and by the association of M-line components (Fulton and Alftine, 1997; Fulton and L'Ecuyer, 1993). Upon this scaffold, Myosin is then integrated to form the thick filaments. In support of this model, the M-line region of Titin is important for myofibrillogenesis (Gotthardt et al., 2003; Musa et al., 2006). The current models of myofibrillogenesis have arisen from studies of cultured cardiomyocytes and in vivo studies have, to date, added little to help resolve between them.

The initial formation of I-Z-I brushes is common between the myofibrillogenesis models and the controversy concerns the assembly and alignment of arrays of I-Z-I brushes and the integration of thick filaments into the nascent sarcomeres. Thick filaments are elaborate structures comprising hundreds of Myosin hexamers in precise alignment with each other and other sarcomeric components. Given this inherent complexity, it is perhaps unsurprising that thick filament assembly is not well understood.

Here we describe the cloning of the *sloth*^{u45} (*slo*^{u45}) mutation and its phenotypic consequences. Zebrafish *slo*^{u45} embryos show no morphological defects and have a normal heartbeat but lack movement of skeletal muscles. Various analyses reveal that the contractility phenotype is due to a lack of assembly of thick

filaments in the nascent sarcomeres of skeletal muscle fibres. Much to our initial surprise, we found that three *slo* alleles all contain mutations in the *hsp90a* (*hsp90a.1* – ZFIN) gene.

Heat-shock proteins (Hsps) are a group of proteins with transcription that is induced in response to heat or other cellular stresses. They are molecular chaperones for huge numbers of proteins and Hsp90 alone may be able to interact with more than 400 different proteins (Zhao et al., 2005). Despite extensive research on Hsps, there has been little work addressing their developmental roles during vertebrate embryogenesis. Work from *C. elegans* has suggested a role for molecular chaperones during thick filament assembly and integration. The Unc45-/Cro1p-/She4p-related (UCS) protein Unc45 functions during assembly of thick filaments (Barral et al., 1998; Barral et al., 2002; Etard et al., 2007) and UNC-45 binds stoichiometrically with Hsp90 (Barral et al., 2002). Our findings extend these studies and show that a single, developmentally regulated *hsp90* gene is necessary for thick filament assembly and for the construction of functional sarcomeres in skeletal myofibrils. Our data reveal unexpected specificity in the developmental role of Hsp90 and raise the possibility that other Hsp genes might play similarly cell-type-specific roles during vertebrate embryogenesis.

MATERIALS AND METHODS

Immunohistochemistry, phalloidin and bungarotoxin staining and in situ hybridisation

Immunohistochemistry was performed by standard methods using: ZNP-1 (DSHB, University of Iowa, IA); anti-Actinin (EA-53; #A5044, Sigma); A4.1025 (Dan-Goor et al., 1990), which recognises all forms of sarcomeric MHC ('pan'-MHC antibody); F59, which is specific to slow-muscle Myosin isoforms (slow-MHC); anti-Titin (T11; Sigma), which marks an epitope in the I-band region of Titin (Fürst et al., 1988). AlexaFluor-conjugated phalloidin or bungarotoxin (Invitrogen) were applied after secondary antibodies. For in situ, DIG-labelled antisense riboprobes were prepared using standard methods from EST constructs (GenBank: *hspa8l*, BI710554; *hsp90a*, CN330912; *unc45b*, CN318309; www.imagenes-bio.de) or from constructs made in-house.

SDS-PAGE and western blotting

Protein was extracted by homogenisation of deyolked embryos and 10 μg of protein was separated using 6% polyacrylamide gels, followed by transfer onto PVDF membrane (Amersham). Myosin antibodies were the same as for immunohistochemistry; rat anti-Hsp90 (16F1, Abcam) was used for Hsp90; mouse anti-γ-Tubulin (Sigma) was the loading control. Peroxidase activity from HRP-conjugated secondary antibodies (Sigma) was detected using an ECL Detection Kit (Amersham).

Electron microscopy

Embryos were fixed in 2% paraformaldehyde, 2% gluteraldehyde in 0.1 M sodium cacodylate buffer (pH 7.3) with 2-5% $CaCl_2$. Tissue was post-fixed in cacodylate-buffered 1% (w/v) osmium tetraoxide, en bloc stained in 2% (w/v) uranyl acetate and embedded in Agar 100 resin (Agar Scientific). Ultrathin sections (80-100 nm) contrasted with saturated uranyl acetate solution and lead citrate were examined and photographed using a JEOL1010 electron microscope.

BAC, DNA rescue and morpholino (Mo) injection

One-cell embryos were injected using capillary needles and Picospritzer II (General Valve) with 10 nl of BAC DNA (RZPD/CHORI; see Table S2 in the supplementary material) made using a BAC Kit (PSI Clone). Full-length u45 mutant and wild-type *hsp90a* were amplified by RT-PCR, cloned into the TOPO vector (Invitrogen) and subcloned by PCR into pCS2myc+. One hundred to two hundred pg of *Sac*II-linearised constructs were injected. Mo sequences were (5′-3′): *hsp90a*, CCGACTTCTCAGGCATCTTGCTGTG; *hsp90a2*, TCGAGTGGTTTATTCTGAGAGTTTC (produced secondary phenotypes) or CTGCTGCTCGTGAGCCTCAGGCATC (GeneTools). 2±0.5 pmoles was injected per embryo.

Microarray analysis

Total RNA was extracted using TRIzol (Invitrogen) from pooled slo^{u45} and wild-type embryos. RNA and microarray processing was carried out at the ICH Gene Microarray Centre (Institute of Child Health, London) according to standard methods. The MAS5 algorithm (Affymetrix) was used to compare wild type and slo^{u45} mutants. Genes designated as showing no change in expression or where expression was designated as absent in both wild type and mutant were eliminated. The data were then split into two groups: genes with a *slo* versus wild-type signal log ratio of between 0.6 and 1 or between –0.6 and –1 (1.5- to 2-fold up- or downregulated) and genes showing a signal log ratio greater than +1 or –1 (greater than 2-fold up- or downregulation). These groups were further sorted into genes absent in wild type or *slo* mutants and those increased and decreased in *slo* mutants (see Table S3 in the supplementary material).

Quantitative PCR (qPCR)

The following cDNA-specific primers (5′-3′) were used for qPCR: *hsp90a* forward (F), CCACCTTAAAGAGGATCAGTCT and reverse (R), TCTTCCTCTTATTCTTGCCAT; *hsp90a2* F, GCGGCGGATCAAAG-AGATC and R, CACTTATCGCCATGATCGTG. cDNA was produced using Superscript II reverse transcriptase (Invitrogen) and 1 μg of quality-checked total RNA extracted using TRIzol from pools of ten mutants and ten wild-type siblings. Triplicate qPCR reactions were carried out with blank controls and five standards. Copy number was determined by reference to standards normalised to a standard curve (ten triplicate 4-fold dilutions); copy number values were normalised to 1 μg of total RNA and significance determined by Student's *t*-test.

Isothermal titration calorimetry, K_d determinations and Hsp90 ATPase assay

The heat of interaction was measured on a MSC System (Microcal), with a cell volume of 1.458 ml, in 20 mM Tris (pH 7.5), 1 mM EDTA, 5 mM NaCl, 7 mM $MgCl_2$ at 30°C. Twenty 14.5 μl aliquots of 1 mM AMPNP were injected into 50 μM yeast Hsp90, human HSP90α or mutant protein. The heat of dilution was determined in a separate experiment by diluting protein into buffer, and the corrected data fitted using a non-linear least square curve-fitting algorithm (Microcal Origin) with three floating variables: stoichiometry, binding constant and change in enthalpy of interaction. ATPase activity of purified mutated and normal yeast and human Hsp90 protein was measured as described previously (Panaretou et al., 1998).

RESULTS

The motility defects of $akineto^{u45}/sloth^{u45}$ mutants are due to defective skeletal muscle fibres

$akineto^{u45}$ is a recessive mutation isolated at UCL in an F3 screen for ENU-induced mutations. Mutant embryos are healthy, show no obvious morphological defects and ostensibly develop as wild-type siblings for their first week. However, they do not move (see Movie 1 in the supplementary material), and die by 8 days post-fertilisation (dpf). Pairwise breeding showed that $akineto^{u45}$ does not complement the tu44c and tm201 alleles of *sloth* (*slo*) (Granato et al., 1996) and we therefore renamed the novel mutation slo^{u45}. *slo* mutants lack spontaneous or stimulus-evoked skeletal muscle contractility but have a normal heartbeat. There is some variability in phenotype between alleles and although no movement is observed in the trunk of homozygous slo^{u45} embryos, the fins of a minority of slo^{u45} mutants show very slight twitching from 4 dpf. By contrast, around 30% of slo^{tu44c} and slo^{tm201} mutants show limited trunk movements at 24 hours post-fertilisation (hpf) that disappear by 48 hpf; by 4 dpf there is substantial, though still compromised, fin movement. Transheterozygotes ($slo^{u45/tu44c}$, $slo^{u45/tm201}$ or $slo^{tu44c/tm201}$) resemble the slo^{tu44c} and slo^{tm201} phenotype, showing some trunk movement at 24 hpf and more vigorous fin twitching later (compared with slo^{u45}). These results suggest that u45, tu44c and tm201 are mutations in the same gene and that u45 is the most severe allele.

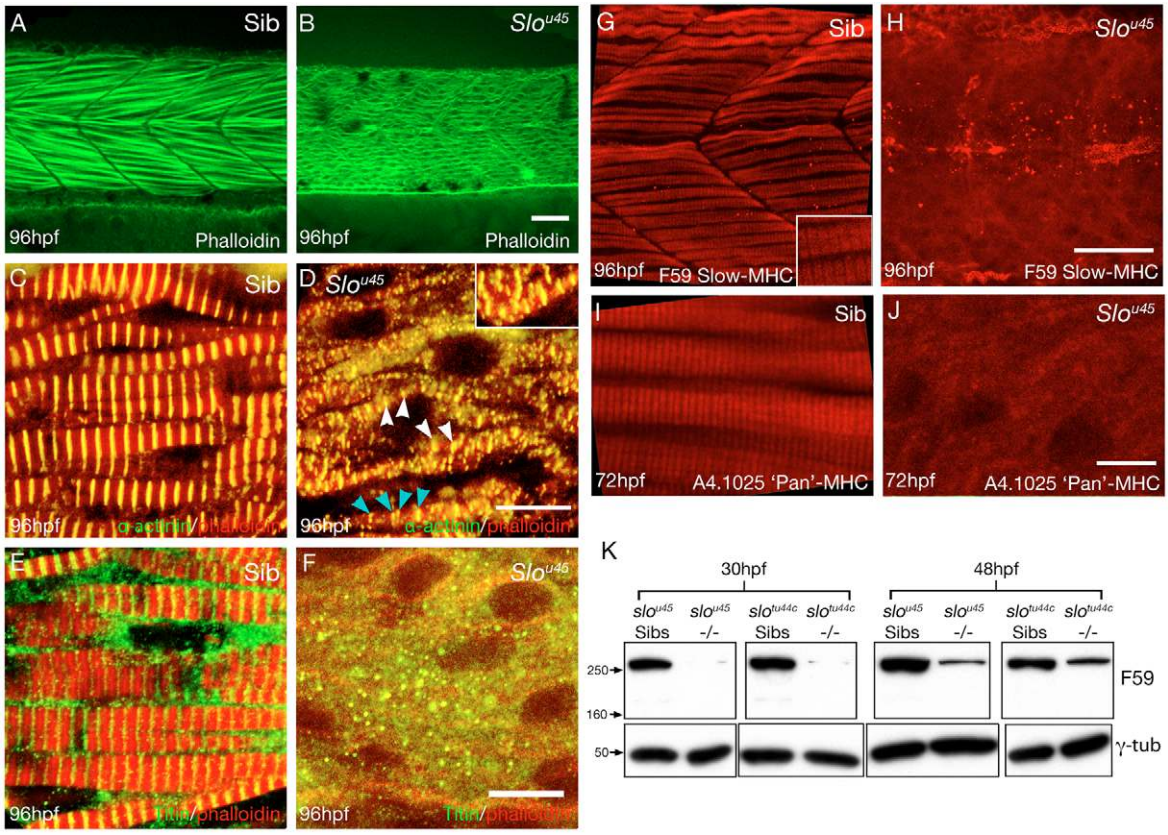

Fig. 1. *slo*^{u45} mutants have disorganised or missing expression of sarcomeric proteins. (**A-J**) Lateral views of muscle fibres in wild-type (Sib) (A,C,E,G,I) and *slo*^{u45} (B,D,F,H,J) zebrafish embryos of ages shown bottom left and with reagents/antibodies shown bottom right. (A,B) F-Actin labelling with phalloidin showing a regular arrangement of fibrils in wild-type muscle fibres, whereas the *slo*^{u45} mutant fibrillar organisation is disrupted. (C,D) Immunohistochemistry for α-Actinin (green) marks the Z-disc, here combined with phalloidin (red); the merge appears yellow. Z-discs are present in the *slo*^{u45} mutant (white arrowheads, D) but are disordered: the distance between Z-discs is irregular (blue arrowheads) and Z-discs from neighbouring fibrils are not in register with each other (inset, D). Z-discs are flanked by Actin filaments in both siblings and mutants. (E,F) Titin labelling (green) using an antibody that marks a region of the molecule around the Z-disc, counterstained with phalloidin (red). (G-J) Immunohistochemistry for MHC (slow muscle Myosin, F59, red in G,H; pan-Myosin A4.1025, red in I,J). In the *slo*^{u45} muscle cells, anti-MHC staining is severely reduced and lacks organisation. (**K**) Western blots using anti-MHC antibody F59 and γ-Tubulin (γ-Tub) as a loading control on lysates of *slo*^{u45} and *slo*^{tu44c} mutant and sibling embryos at 30 hpf and 48 hpf. MHC protein levels are reduced in mutants of both alleles. Scale bars: 20 μm in A,B,G,H; 10 μm in C-F; 8 μm in I,J.

The two most likely causes of the *slo* phenotype are defective innervation of muscle fibres and/or a defective contractile response of the muscle fibres to innervation. Examination of muscle innervation and calcium transients within muscle fibres revealed only minor differences between *slo*^{u45} mutants and wild types (see Fig. S1 and Table S1 in the supplementary material). The absence of neuronal or excitation-coupling problems suggested a defect intrinsic to the muscle fibres. This was corroborated by polarised microscopy, mosaic labelling and cell transplantation experiments which showed that *slo*^{u45} mutants had abnormally wavy muscle fibres that totally lacked birefringence (see Fig. S1 in the supplementary material). This strongly suggested a defect intrinsic to the contractile apparatus of the muscle fibres.

The filamentous organisation of myofibrils is abnormal in *slo* mutants

Antibodies and probes for sarcomeric components elucidated the sarcomeric defects underlying the myofibrillar phenotype of *slo*^{u45} embryos (Fig. 1). We found that although filamentous Actin is present, the myofibrils of *slo*^{u45} mutants lack the organised fibrillar arrangement seen in siblings (Fig. 1A,B). Sarcomeric filamentous Actin is anchored at Z-discs composed of α-Actinin, capping proteins and other molecules. Double staining for Z-discs and Actin filaments in siblings revealed evenly spaced Z-discs in register between neighbouring fibrils and even between adjacent fibres (Fig. 1C). *slo*^{u45} myofibrils lacked such regimented organisation (Fig. 1D). Much of the anti-Actinin staining was dispersed in the cytoplasm, although small structures resembling Z-discs surrounded by Actin were present. However, these mutant 'Z-discs' were neither appropriately spaced nor in register. The sarcomeric organisation of Titin evident in siblings was absent in *slo*^{u45} mutants (Fig. 1E,F), and although some Titin-positive puncta were present in the *slo*^{u45} mutants, they showed little evidence of organisation.

Anti-MHC immunoreactivity was considerably reduced in *slo*^{u45} mutants. Unlike in siblings, the muscle of *slo*^{u45} mutants lacked strong anti-MHC labelling, with no signs of striations in register between neighbouring fibres (Fig. 1G-J). Consistent with its less severe movement phenotype, MHC immunohistochemistry in the tu44c allele revealed short lengths of striation (see Fig. S2A,B in the supplementary material).

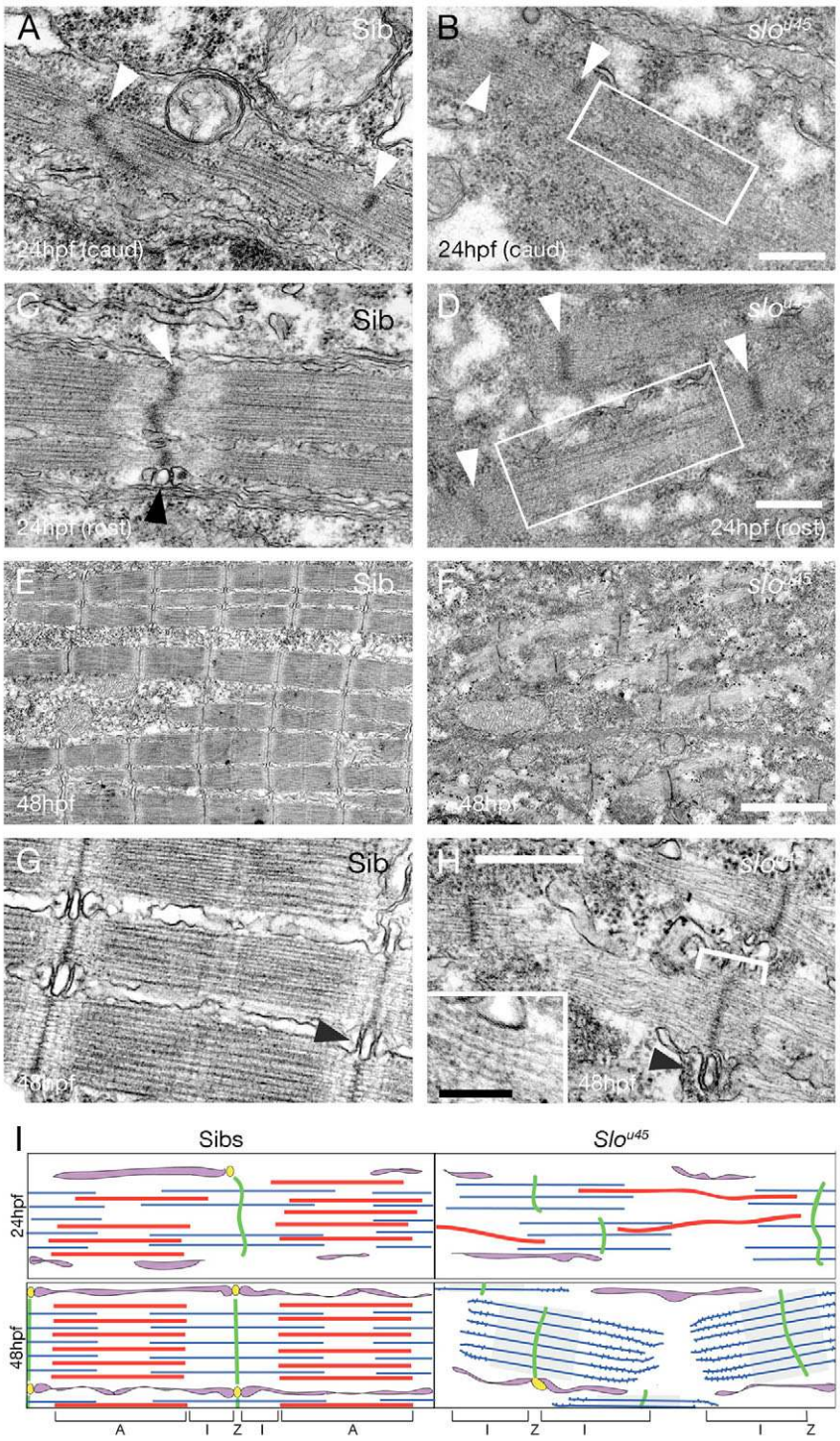

Fig. 2. Sarcomeres in *slo*^{u45} mutant myofibrils lack thick filaments. (**A-H**) Electron micrographs of sarcomeres from wild-type (Sib) (A,C,E,G) and *slo*^{u45} mutant (B,D,F,H) myofibrils at the ages shown bottom left. (A,B) Caudal myotomes of 24 hpf zebrafish embryos. White arrowheads (A) show immature Z-discs with poorly positioned thick and thin filaments. In *slo*^{u45} mutants, bundles of thin filaments are present with putative early Z-discs (B, arrowheads). Very rarely, structures of dimensions approximating to those of thick filaments were present (box, B). (C,D) Rostral myotomes of 24 hpf embryos. The wild type has recognisable sarcomeres with almost straight Z-discs (white arrowhead, C) and more fully formed sarcoplasmic reticulum with triads (black arrowhead, C). In the *slo*^{u45} mutant, I-Z-I brushes are formed [Z-discs (white arrowheads, D) flanked on either side by thin filaments], and a few putative thick filaments are evident (box, D). (E-H) At 48 hpf, wild-type muscle fibres are packed with mature myofibrils (E,G), possessing mature triads at each Z-disc (black arrowhead, G). Mutant muscle fibres contain no thick filaments but numerous I-Z-I brushes are evident (F,H). The Z-lines are surrounded by an electron-dense region (bracket, H; F); beyond this region the thin filaments have light striations on them (see inset, H). Triads are present, although less common (black arrowhead, H). (**I**) Schematic summarising the principal differences between *slo*^{u45} mutant and sibling sarcomere ultrastructure. At early stages of myofibrillogenesis (top), mutants have less numerous and malformed thick filaments (red), and I-Z-I brushes (green and blue) are present but less well aligned than siblings. By 48 hpf, wild-type sarcomeres are fully formed, whereas in mutants only misaligned and mis-spaced I-Z-I brushes with striated thin filaments are present (blue). T-tubules and sarcoplasmic reticulum are shown in yellow and purple, respectively. Scale bars: 500 nm in A-D,G,H; 2 μm in E,F; 100 nm in H inset.

Western blots showed that MHC was almost completely absent from lysates of *slo* mutants at 30 hpf, when myofibrils are initially forming. By 48 hpf, when the majority of muscle fibres contain mature fibrils, Myosin levels had increased slightly in *slo* mutants although not near to levels in sibling lysates (F59, Fig. 1K; A4.1025, data not shown). These results suggest that either thick filaments are not formed because of a lack of Myosin, or that Myosin is degraded because thick filaments do not form correctly.

slo myofibrils are deficient in thick filaments

To examine more closely the defects in the contractile apparatus of *slo*^{u45} muscle, we used transmission electron microscopy (TEM) to visualise the sarcomeric machinery at 24 hpf (Fig. 2A-D), when movement is just beginning, and at 48 hpf (Fig. 2E-H), when coordinated movement is present.

In less mature caudal myotomes of wild-type 24 hpf embryos, myofibrils were rare and those present were very immature. Z-discs were small in diameter and poorly aligned, thick and thin filaments

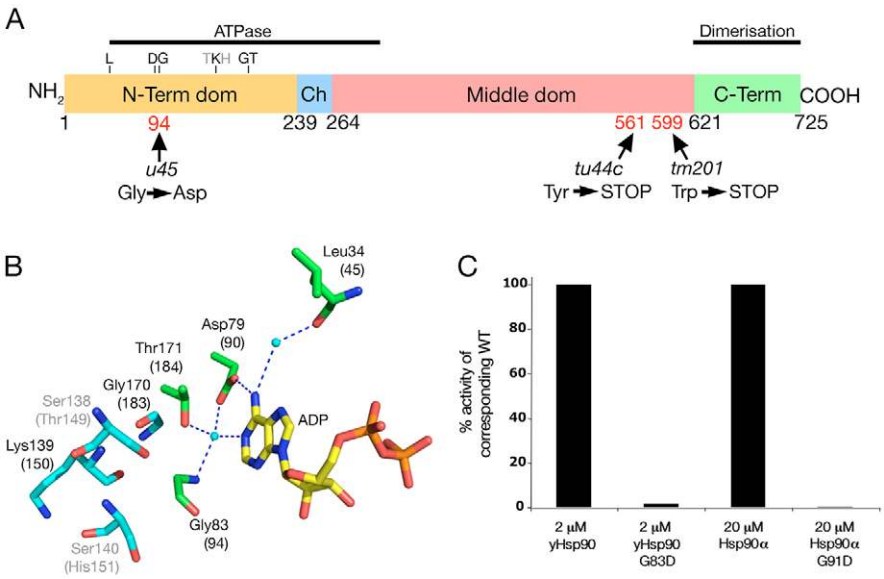

Fig. 3. The ATPase activity of Hsp90 is abrogated by the *slo*^{u45} mutation. (**A**) Hsp90a domain structure (amino acid numbers of domain boundaries are shown beneath; known functions of regions are indicated by black bars). The positions and consequences of mutations in three *slo* alleles, u45, tu44c and tm201, are also illustrated beneath. The equivalent residue locations of yeast Hsp90 as represented in B are shown above. (**B**) Pymol diagram showing critical binding interactions of ADP with yeast Hsp90. Dotted blue lines are hydrogen bonds; amino acid residues (corresponding residue numbers in zebrafish are in parentheses and are also indicated in A) involved are in green; water molecules are cyan balls; residues packed against the C-α atom of Gly83 are shown in cyan. Illustrated residues are conserved between yeast and zebrafish, except Ser138/Thr149 and Ser140/His151 (grey), which are conservative substitutions unlikely to cause major structural changes. Binding of ATP/ADP to the Hsp90 N-terminal domain involves highly conserved interactions including the carboxylate side-chain of Asp79 and main-chain carboxyl of Leu34, via a tightly bound water molecule, to the exocyclic N6 of adenine. The same Asp79 also interacts via another tightly bound water to the N1 imino-nitrogen of the adenine. This same water is bound by an interaction with the side-chain hydroxyl of Thr171 and main-chain amide of Gly83. An aspartic acid residue substitution at Gly83 (mimicking the u45 mutation) would lead to steric clashes likely to disrupt critical hydrogen bonding interactions with ADP/ATP. (**C**) ATPase activity of yeast Hsp90, human HSP90α and their u45-mimic mutants. ATPase activity of the yeast G83D and human G91D mutants is negligible relative to corresponding wild type.

were present but were few in number and were not yet organised into A and I bands (Fig. 2A). Structures resembling myofibrils were essentially absent from *slo*^{u45} mutants (Fig. 2B). Where a presumptive nascent sarcomere could be found, it comprised small aggregations of thin filaments sometimes associated with densities (putative Z-discs).

In more mature rostral myotomes of 24 hpf wild types, myofibres often contained one or two almost complete myofibrils; such structures were absent from *slo*^{u45} fibres (Fig. 2C,D). Although more fully constructed than their caudal counterparts, these structures were still immature in wild-type embryos. Z-discs were not straight and thick filaments were sporadic and not fully integrated. In *slo*^{u45} mutants, the rostral myotomes contained some thin filament/Z-disc aggregates with Z-discs usually forming isolated 'I-Z-I brushes'. Occasionally, a few spindly thick-filament-like structures were present, appearing to lace together adjacent I-Z-I brushes.

By 48 hpf, wild-type myofibres contained multiple highly organised myofibrils with Z-discs in register, whereas *slo*^{u45} myofibres contained only disorganised I-Z-I brushes (Fig. 2E,F). These were often found in groups with the Z-discs only partially in register with their neighbours and the distance between consecutive I-Z-I brushes was also highly variable. Thick filaments were absent from *slo*^{u45} myofibrils. Either side of the Z-disc was an electron-dense area, 100-200 nm wide, within which the bundle of I-band thin filaments retained the same height as the Z-disc. Beyond this region, the bundles of thin filaments were slightly striated and narrower than the diameter of the Z-disc (Fig. 2G,H). The periodicity of the striations was approximately 30 nm, suggesting that they could be Troponin complexes that would normally interact with Myosin heads (Chun and Falkenthal, 1988).

The ultrastructural appearance of *slo*^{tu44c} muscle was broadly similar to *slo*^{u45} mutants, with I-Z-I brushes lacking thick filaments. However, the I-Z-I brushes were more regularly spaced and aligned with short disorganised fibrous aggregations of electron-dense material between I-Z-I brushes (see Fig. S2 in the supplementary material). It is probable that these aggregates correspond to the striations seen with MHC immunohistochemistry.

The heart of *slo*^{u45} mutants functions normally and, unsurprisingly, the ultrastructure of the heart muscle was indistinguishable between *slo*^{u45} mutants and siblings (see Fig. S3 in the supplementary material).

These ultrastructural observations (summarised in Fig. 2I) reveal that the cause of the *slo* phenotype is a failure to assemble and integrate thick filaments into the nascent sarcomeres of myofibrils. Actin (thin) filaments and Z-lines (containing Actinin) are present, as is the excitation-coupling apparatus of T-tubules and sarcoplasmic reticulum. However, I-Z-I brushes fail to align and they lack regular spacing. The lack of aligned thick filaments underlies the birefringence deficiency and lack of organisation observed in the Myosin immunohistochemistry. Therefore, the Slo protein is not required to form a Z-disc and to assemble Actin fibres, Actinin and probably other sarcomeric proteins, but is required for assembly and integration of thick filaments.

slo mutations are in the *hsp90a* gene

Genetic mapping using SSLP markers placed the *slo* locus on LG20 (see Fig. S4 in the supplementary material). Bespoke SNP markers for genes in this region showed tight linkage to *hsp90a*, which is immediately adjacent to *hsp90a2* (*hsp90a.2* – ZFIN). Sequencing of these genes from the three mutant *slo* alleles revealed mutations in *hsp90a* (Fig. 3A and see Fig. S4 in the supplementary material). A guanine to adenine point mutation is present in exon 3 in *slo*^{u45} mutants, causing a glycine to aspartic acid change in residue 94. In exon 9 of *slo*^{tu44c} and exon 10 of *slo*^{tm201}, there are point mutations that respectively change tyrosine 561 and tryptophan 599 to stop codons. No mutations were found in *hsp90a2* coding sequence in any *slo* allele.

The nonsense *slo*^{tu44c} and *slo*^{tm201} mutations would result in truncated molecules missing the C-terminal domain, which is important for both homo- and heterodimerisation (Ali et al., 2006); such truncations would have severe functional consequences for the molecule.

The molecular consequence of the *slo*^{u45} missense mutation was initially less obvious, but bioinformatic analysis and further experiments demonstrated that it abrogates the ATPase function of the Hsp90a protein. The N-terminal region of Hsp90 harbouring the mutation is required for ATP hydrolysis (Panaretou et al., 1998), and a ClustalW alignment of available Hsp90a sequences demonstrated the glycine mutated in *slo*^{u45} to be universally conserved (see Fig. S5 in the supplementary material). To predict the functional consequences of the Gly to Asp change, we assessed its probable consequence on the protein structure of yeast Hsp90, for which the crystallographic structure was available (Ali et al., 2006) (Fig. 3B). The C-α atom of Gly83 sits in a confined space that is 3.4 Å from the hydroxyl of Ser138, 3.8 Å from the main-chain carbonyl of Lys139, 3.9 Å from the main-chain carbonyl of Gly170, and 4.4 and 4.8 Å from the main-chain amides of Gly170 and Lys139, respectively (Fig. 3B). The large side-chain of an aspartic acid residue would not be easily accommodated and would disrupt the local folding of the protein. As the glycine is involved in critical interactions with bound ATP/ADP, it is highly likely that the side-chain change would severely affect the ability of mutant Hsp90 to bind nucleotide.

To test directly whether a Gly to Asp mutation at this site affects ATPase function, we recapitulated the mutation in yeast and human forms and tested their ATPase and ATP-binding properties in vitro. The mutations completely abrogated the ability of these molecules to hydrolyse ATP (Fig. 3C). Binding between the ATP analogue AMPPNP and mutant yeast and human Hsp90 was also negligible (see Fig. S6 in the supplementary material). Functional ATPase activity is essential for chaperoning by Hsp90 (Panaretou et al., 1998; Pearl and Prodromou, 2006). The *slo*^{u45} mutation is therefore catastrophic for the function of zebrafish Hsp90a as a chaperone.

The *slo* phenotype is rescued by exogenous Hsp90a

To confirm that the mutations identified above were indeed the cause of the muscle defects in *slo* mutants, we attempted to rescue the phenotype. Several BACs that covered the genomic region (see Fig. S4, and also Table S2 for clone names, in the supplementary material) were injected into batches of embryos from crosses of *slo*^{u45} or *slo*^{tu44c} heterozygotes. At 3 dpf, injected embryos showed normal movement, partial movement or paralysis (Table 1 and see Movie 2 in the supplementary material). Examination of muscles from partially moving embryos with polarised light revealed a mosaic pattern of birefringence in the myotomes (see Fig. S4 in the supplementary material), indicating that some cells, most likely those containing mosaically inherited BAC DNA, had functional myofibrillar assemblies. Although *hsp90a* and *hsp90a2* are separated by only 2 kb, we found two BACs (8 and 9) with ends in this 2 kb region facing in opposite directions, thus separating the two genes. Injection of BAC 9 (*hsp90a* only) produced mosaically rescued embryos, as expected. Surprisingly, BAC 8 (*hsp90a2* only) also rescued some embryos (Table 1), albeit less efficiently, suggesting that exogenous Hsp90a2 can partially compensate for loss of Hsp90a.

A caveat to these rescue experiments is that BACs contain more than one gene and so one cannot be certain that the rescue is due to the activity of a single gene. To address this issue, we co-injected morpholinos (Mos) against *hsp90a* or *hsp90a2* along with the corresponding BAC. In both cases, the ability of the BACs to rescue movement of *slo*^{u45} embryos was blocked, confirming that it is the activity of the Hsp90 proteins that mediates rescue. Additionally, *hsp90a* Mo produces immotile embryos lacking birefringence (Table 1); conversely, neither of two *hsp90a2* Mos disrupted muscle function [data not shown and see Etard et al. (Etard et al., 2007)].

The *slo*^{u45} allele is a missense mutation and, despite our study of the yeast and human mutant proteins, we could not be certain (1) that it is an amorphic (or weakly antimorphic) mutation in the zebrafish and (2) that the mutation is responsible for the lack of thick filaments. Therefore, to determine if the mutant protein has any residual activity in myofibrillogenesis, we assayed whether exogenous mutant protein could rescue movement and thick filament generation. Constructs encoding N-terminal myc-tagged wild-type (*myc:WThsp90a*) and u45 mutant (*myc:u45Hsp90a*) Hsp90a were injected into *slo*^{u45} mutants. Only the *myc:WThsp90a* construct rescued movement in *slo*^{u45} mutants. Mosaically distributed myc:WTHsp90a-expressing muscle cells in *slo*^{u45} mutants possessed apparently normal levels of organised Myosin and resembled wild-type muscle fibres transplanted into *slo*^{u45} embryos (Fig. 4A-D and see Fig. S1K in the supplementary material), indicating a rescue of thick filament formation. Muscle cells in *slo*^{u45} mutants expressing the myc:u45Hsp90a protein had neither higher levels of Myosin immunoreactivity nor organisation in the Myosin present at low level (Fig. 4F). Sibling muscle fibres

Table 1. Exogenous *hsp90* rescues the *slo* phenotype

		Injected embryos				Non-injected control			
Construct	*slo* allele	Normal	Partial	Paralysed	*n*	Normal	Partial	Paralysed	*n*
BAC 2	u45	73.3	14.4	12.3	146	76.2	0	23.8	126
BAC 4	u45	74.7	16.9	8.4	83	80.5	0	19.5	113
BAC 5	u45	77.2	21.5	1.3	79	77.2	0	22.8	127
BAC 6	u45	75	21.7	3.3	60	81.9	0	18.1	72
BAC 8 (*hsp90a2*)	u45	83.1	9.6	7.2	83	73	0	27	74
BAC 8 (*hsp90a2*)	tu44c	75.7	6.5	17.8	185	78.3	0	21.7	230
BAC 8 + hsp90a2MO	tu44c	71.6	0	28.4	81	75	0	25	88
BAC 9 (*hsp90a*)	u45	72.7	25.5	1.8	55	76.3	0	23.7	59
BAC 9 (*hsp90a*)	tu44c	79	11.2	9.8	143	77.6	0.6	21.8	174
BAC 9 + hsp90aMO	tu44c	0	2.9	97.1	35	–	–	–	–

Percentages of paralysed embryos and those showing normal and partial movement after injection with BACs, BACs plus Mos, and in non-manipulated populations.

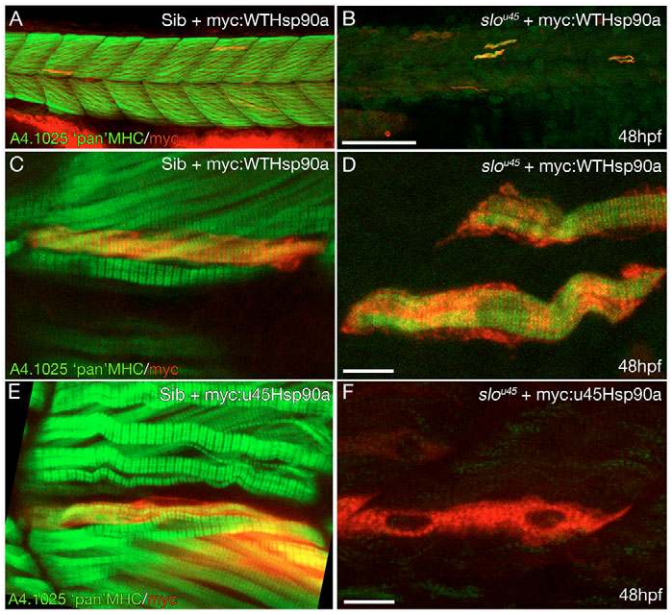

Fig. 4. Wild-type Hsp90a rescues thick filament formation in *slo*^{u45} muscle cells whereas Hsp90a^{u45} does not. (**A-D**) Muscle fibres from a *slo*^{u45} mutant (B,D) and wild-type (Sib) (A,C) injected with DNA encoding myc:WTHsp90a double stained for myc (red) and MHC (green). MHC staining in siblings decorates the cells with organised bands (C) indicative of mature A-bands. In the *slo*^{u45} mutant, striations in the MHC staining are only evident in myc+ cells (D). (**E**,**F**) Muscle fibres in sibling embryos injected with myc-tagged *hsp90a*^{u45} DNA show organised MHC staining of myc+ cells (E). Myc+ cells in *slo*^{u45} mutants injected with the same construct do not show organised myofibrils (F). Scale bars: 100 μm in A,B; 10 μm in C-F.

expressing myc:u45hsp90a retained the ability to express Myosin in orderly myofibrils, suggesting that the u45 mutant Hsp90a does not have detectable antimorphic activity (Fig. 4E).

The *slo*^{u45} missense allele gives a slightly stronger contractility phenotype and more severe disruption to myofibrillogenesis than the truncated *slo*^{tu44c} allele (Figs 1, 2 and see Fig. S2 in the supplementary material), and we assayed whether this might be due to enhanced activity of the *hsp90a2* gene in the tu44c background. However, Mo-based abrogation of Hsp90a2 activity in *slo*^{tu44c} mutants failed to block muscle twitches. This suggests that the *slo*^{tu44c} mutant Hsp90a protein retains a residual ability to mediate myofibrillogenesis. This is probably due to function of the intact ATPase region and as the dimerisation domain is missing in this allele, it suggests that the Hsp90 monomer retains some activity. Altogether, these results confirm that *hsp90a* is the gene affected by the *slo* mutations and that Hsp90a has a unique and specific developmental role in the assembly and integration of thick filaments onto nascent sarcomeres of skeletal muscle.

hsp90a and genes encoding proteins that may interact with Hsp90a to mediate sarcomere assembly are upregulated in *slo* mutants

Using Affymetrix arrays, we compared mRNA expression profiles of wild-type and *slo*^{u45} embryos (see Tables S3, S4 in the supplementary material). Amongst the genes with lowered levels of expression were several encoding sarcomeric proteins, including Myosin light chains, Titin and Troponins. Notably, several genes encoding heat-shock proteins and factors that interact with heat-shock proteins were upregulated. *hspa8l* and a similar gene homologous to human *HSPA1A*/*HSPA1B* showed the largest *slo*^{u45} versus wild-type differences, with 150- to 160-fold upregulation in mutants. Both *hsp90a* and *unc45b*, a gene proposed to interact with Hsp90 during myofibrillogenesis (Barral et al., 2002; Etard et al., 2007), were 4-fold upregulated in mutants. For selected genes, in situ hybridisation (ISH) analysis corroborated the expression changes found using the microarray. *hspa8l* was massively upregulated in the myotomes of both *slo*^{u45} and *slo*^{tu44c} mutants (Fig. 5A-C), whereas both *unc45b* and *hsp90a* showed more modest increases in ISH signal in *slo*^{u45} mutants (Fig. 5D-I). In surprising contrast to the upregulation of *hsp90a* in *slo*^{u45} embryos and *hsp90a* morphants (see Fig. S8 in the supplementary material), *hsp90a* transcript levels were reduced in *slo*^{tu44c} mutants (for which no microarray analysis was carried out), despite upregulation of both *unc45b* and *hspa8l* in the morphant and both mutant alleles (Fig. 5C,F,I and see Fig. S8 in the supplementary material). Complementing the changes at the mRNA level, western blot analysis revealed that Hsp90 protein levels were increased in *slo*^{u45} mutants and decreased in *slo*^{tu44c} mutants when compared with siblings (Fig. 5J).

In summation, these results show that when Hsp90a function is compromised, as in *slo*^{u45} mutants, levels of transcription of genes encoding certain sarcomeric proteins are reduced, whereas expression levels of genes that encode several chaperone and co-chaperone proteins (*hspa8l*, *hsp90a*, *unc45b* and others) are upregulated (with the allele-specific exception of *hsp90a* in *slo*^{tu44c} mutants).

Hsp90a2 has no role in myofibrillogenesis

Our data have revealed a requirement for *hsp90a* in myofibrillogenesis, but not for its neighbouring *hsp90a2* gene. The reasons why *hsp90a2* appears to have little or no role in muscle were not clear and so we designed experiments to assess expression of *hsp90a2* and further explore its function (or lack of function). ISH analysis suggests that, like *hsp90a*, *hsp90a2* is expressed in muscle tissue but expression levels are low (data not shown) (Etard et al., 2007). However, as expression was low and to strengthen these data, quantitative RT-PCR (qPCR) was performed to examine the differences in levels of mRNA for *hsp90a* and *hsp90a2* in wild-type and *slo* embryos (u45 and tu44c alleles).

hsp90a expression levels were significantly increased in *slo*^{u45} mutants compared with siblings (Fig. 5K), whereas expression levels of *hsp90a2* were unaffected by either mutation (Fig. 5L). This indicates that although the genes are adjacent to each other, they are subject to differential transcriptional regulation. This conclusion is supported by analysis of the absolute levels of transcription of the two genes in wild-type embryos, with *hsp90a* expression nearly eight times that of *hsp90a2* (Fig. 5K,L; see Fig. S7 in the supplementary material). This offers a likely explanation for why endogenous *hsp90a2* does not compensate for mutations in *hsp90a*. Presumably, the low expression level of *hsp90a2* that fails to be upregulated as a consequence of mutation in *hsp90a* means that there is very little Hsp90a2 activity in developing muscle of either wild-type or *slo* embryos. By contrast, the expression level of *hsp90a2* following BAC injection is presumably sufficiently high to mediate partial rescue. Supporting the conclusion that *hsp90a2* has no role in muscle development, *hsp90a2* morphants show normal birefringence of muscle fibres and fail to upregulate *hsp90a*, *unc45b* or *hspa8l*, and the phenotype of *hsp90a*/*hsp90a2* double morphants is no more severe than that of *hsp90a* and *hsp90a2* single mutants/morphants [see Fig. S8 in the supplementary material and Etard et al. (Etard et al., 2007)].

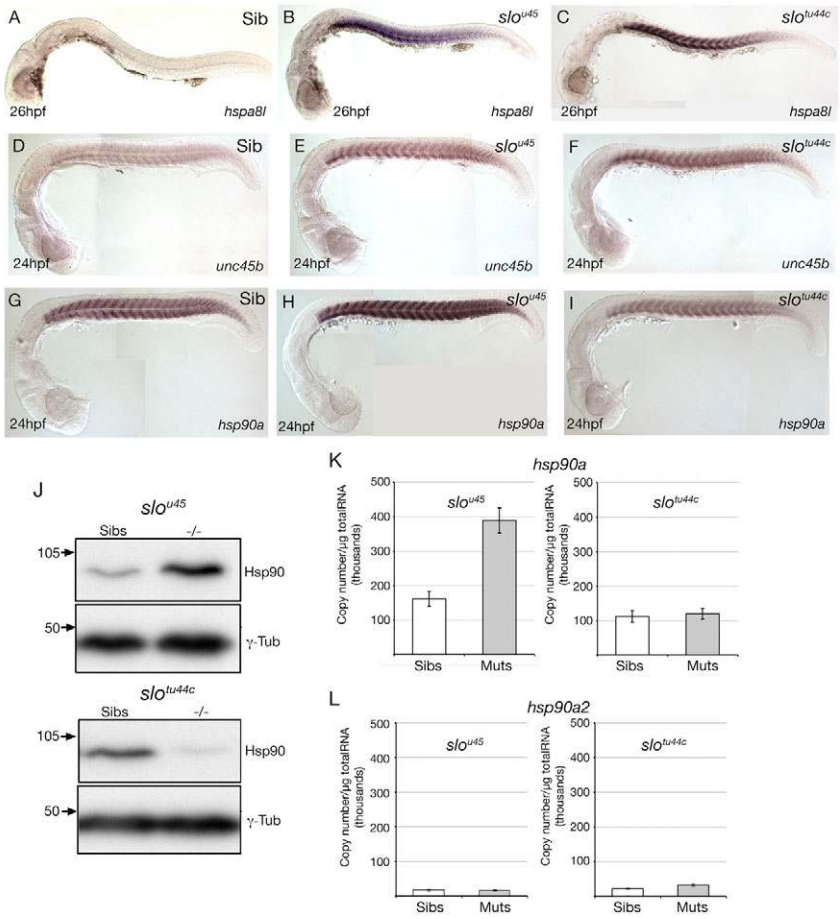

Fig. 5. Abrogation of *hsp90a* but not *hsp90a2* function leads to upregulation of genes encoding proteins likely to be involved in sarcomere assembly. (**A-I**) Lateral views, at the stage indicated bottom left, showing expression of the genes indicated bottom right in wild-type (Sib) and mutant zebrafish embryos. Note that although *hspa8l* and *unc45b* are upregulated in the *slo*^{tu44c} allele, *hsp90a* itself is not. (**J**) Western blots using lysates of *slo*^{u45} and *slo*^{tu44c} mutant and sibling embryos. More Hsp90 protein was present in *slo*^{u45} mutant lysates than in the corresponding siblings. By contrast, *slo*^{tu44c} mutant lysates contained less Hsp90 protein than siblings. (**K**,**L**) Quantitative PCR (qPCR) analyses of levels of *hsp90a* and *hsp90a2* expression in wild type (Sibs), *slo*^{u45} and *slo*^{tu44c} mutants (Muts). Absolute expression levels of *hsp90a* (normalised to μg of total RNA) were significantly increased (K; P=0.002, n=5) in *slo*^{u45} mutants compared with siblings; levels of expression of *hsp90a* in *slo*^{tu44c} mutants were unchanged compared with siblings (K; P=0.75, n=3); and levels of expression of *hsp90a2* were not significantly different between *slo*^{u45}mutants and siblings nor between *slo*^{tu44c} mutants and siblings (L; P=0.813, n=5 and P=0.074, n=3, respectively).

DISCUSSION

slo mutants exhibit a developmental phenotype specifically affecting skeletal muscle myofibrillogenesis. Within *slo* mutant myofibres, the initial steps in construction of sarcomeres are relatively normal, leading to formation of Actin-filament-decorated Z-bands. However, these I-Z-I brushes fail to align or become properly spaced and nascent sarcomeres lack properly formed thick filaments. The level of MHC protein is reduced in mutants, suggesting that Myosin protein is degraded. Four main lines of evidence indicate that this phenotype is due to mutations in *hsp90a*: (1) mutations are found in three *slo* alleles; (2) the phenotype is rescued by exogenous wild-type Hsp90 and is (3) phenocopied by *hsp90a* Mo; and (4) the transcriptional upregulation of *hsp90a* and *hspa8l* (a *hsp70*-related gene) is a conserved response to the loss of Hsp90a activity (Blagg and Kerr, 2006). Moreover, structural and functional analysis of the u45 mutation indicate that it is the ATPase-dependent chaperoning activity of Hsp90 that is important for thick filament formation and integration.

The developmental requirement for *hsp90a* is restricted to skeletal muscle cells

Given the vast amount of literature on roles for Hsp90 in many cellular events, we were initially surprised to find such a specific role for *hsp90a* during embryonic development. Little has been published on the requirements for Hsps during normal developmental processes in vertebrates, so the issue of tissue and cell-type specificity of function has not previously been addressed.

Two possible explanations for the specificity of the *hsp90a* mutant phenotype are either that skeletal muscle is the only embryonic cell type to require Hsp90 activity, or that other *hsp90* genes function in other developing cells. In favour of a specific requirement in skeletal muscle cells, construction of the myofibrillar apparatus is an enormous challenge to the machinery of the cell, and muscle cells probably have the greatest load of any developing cell type in terms of protein folding and construction of multimeric protein complexes. To build a sarcomere requires balancing of the transcription, translation and folding of proteins and their incorporation into reiterative sarcomeric units. In this context, the demands upon protein chaperones will be high so Hsp90a might have been recruited for this specific developmental role. Additionally, given the large numbers of Hsp genes, it is almost certain that others will have developmental roles. With respect to *hsp90a* genes, in zebrafish there are at least three – *hsp90a*, *hsp90a2* and *hsp90ab1* (formerly *hsp90b*) (Krone et al., 1997) – raising the possibility that different paralogues function in different developmental events.

Hsp90a may co-operate with Unc45 in the chaperoning of Myosin during myofibril assembly

Hsp90s are well-characterised molecular chaperones with diverse and wide-ranging roles in cellular physiology (Pearl and Prodromou, 2006). The current hypothesis for the chaperoning role of the Hsp90 homodimer is that the N-terminus ATPase domain flexes upon binding of ATP and this facilitates the maturation of client proteins (Ali et al., 2006; Pearl and Prodromou, 2006).

Although this hypothesis suggests how Hsp90 chaperones, it does not explain how client specificity is managed (Pearl and Prodromou, 2006). Unlike many chaperones, Hsp90 shows much specificity for the proteins it binds, although these client proteins are very diverse and may number over 400 (Zhao et al., 2005). With this specific, yet potentially wide-ranging network of interactions, it is perhaps all the more surprising that *slo* mutants only show defective skeletal thick filament formation. By what mechanisms might Hsp90a specifically act to chaperone Myosin during thick filament formation?

Substrate-specific binding sites in the middle domain of the Hsp90 molecule, in addition to recruitment of various co-chaperone molecules, may contribute to the client specificity of the chaperoning activity (Pearl and Prodromou, 2006). Included among co-chaperones is the UCS-factor Unc45, identified through a *C. elegans* screen as being required for muscle development (Barral et al., 1998; Venolia et al., 1999). These studies led to the proposition that Unc45 acts in concert with Hsp90 to chaperone Myosin. In a recent study Etard et al. demonstrated that the *steif* zebrafish motility mutant is due to mutations in the *unc45b* gene and that Steif/Unc45b binds Hsp90 (Etard et al., 2007). These results point to a highly conserved mechanism whereby Unc45 provides specificity with Hsp90 for chaperoning Myosin during myofibrillogenesis.

The regulation of *hsp90a* during skeletal muscle development is likely to be independent of the normal heat-shock response pathway

During the course of our studies, we made several observations regarding the regulation of mRNAs and proteins in wild-type and *slo* muscles: we find that *hsp90a* is strongly expressed in wild-type skeletal muscle; that both *hsp90a* mRNA and Hsp90 protein and *hspa8l* and *unc45* mRNA levels are increased in slo^{u45} mutants whereas *hsp90a2* is not; that *hsp90a* mRNA is not upregulated and Hsp90 protein levels are lower in slo^{tu44c} mutants; that Myosin protein levels are severely reduced in slo^{u45} mutants; and that genes encoding several sarcomeric proteins are downregulated in slo^{u45} mutants. Do these observations make sense and shed any light on the transcriptional and post-translational mechanisms that operate during sarcomere assembly?

There are two obvious possibilities to explain the strong tissue-specific expression of *hsp90a* during normal skeletal muscle development. The first is that the stress levels that occur in developing myofibres induce the 'heat-shock response', a well-established trigger for upregulation of *hsp90* transcription. The second is that the high-level expression of *hsp90a* in skeletal muscle cells is developmentally regulated, independent of the heat-shock regulation of *hsp90a* transcription. We favour this second possibility as our data suggest that the heat-shock response is not triggered during normal muscle development, whereas it is triggered in *slo* mutant muscle cells.

A well-established signature for reduced Hsp90 function is the upregulation of *hsp90*- and *hsp70*-related genes and the ubiquitination and proteosome-mediated destruction of Hsp90 client proteins (Proisy et al., 2006). In such situations, it is thought that the depletion of Hsp90 (through cellular-stress-induced client binding, mutations or for other reasons) frees the transcription factor Hsf (Heat shock factor), which triggers the heat-shock response through upregulation of various Hsp genes. Thus, the upregulation of chaperone genes and depletion of client proteins (Myosin) in *slo* mutants are entirely consistent with the muscle cells mounting a stress response owing to loss of Hsp90a function.

In contrast to the situation in *slo* mutants, there is no indication that the expression of *hsp90a* during normal development is a direct consequence of the cell mounting a stress response. Perhaps most notably, *hspa8l* expression is virtually undetectable in wild-type developing muscle in contrast to *slo* mutant muscle. Thus, it seems much more likely that an alternative, developmentally regulated transcriptional mechanism leads to upregulation of *hsp90a* during normal myogenesis. This would, in principle, not be difficult to achieve as various muscle-specific transcription factors are active during the period of myofibrillogenesis (Hinits and Hughes, 2007).

The reduction in Myosin protein levels in slo^{u45} and slo^{tu44c} mutants could be explained by the well-established proteasome-mediated degradation of Hsp90 client proteins in the absence of Hsp90 function (Blagg and Kerr, 2006). We have no explanation for the reduced transcription of other genes involved in myofibrillogenesis, although this suggests a feedback mechanism balancing transcription levels with the translation and further processing of sarcomeric proteins.

It is curious that slo^{tu44c} mutants show upregulation of *unc45* and *hspa8l*, but not *hsp90a* itself. The fact that tu44c is a nonsense mutation might lead to nonsense-mediated mRNA decay and, if this happens, to a lowering of transcript and protein levels. However, it does not seem likely that mRNA decay would completely mask the strong constitutive expression that should be induced by the stress response. The milder phenotype of slo^{tu44c} and $slo^{u45/tu44c}$ mutants suggests that some translation does occur and that the Slo^{tu44c} Hsp90a protein retains some function, presumably in its N-terminal portion. It might still retain the ability to sequester Hsf and hence a milder stress response may be mounted in the mutant muscle cells. However, this does not really explain why *unc45* and *hspa8l* respond similarly in both mutant alleles. Finally, one should also consider that the truncated $Hsp90^{tu44c}$ protein might in some unknown way suppress the *hsp90a* transcriptional upregulation response.

It is also curious that despite being located adjacent to *hsp90a*, *hsp90a2* is subject to different transcriptional regulation and has no obvious role in muscle formation. Given their proximity and similarity in sequence, it seems likely that the two genes arose through a tandem duplication event. *hsp90a2* still encodes a functional protein and so it must retain a function in zebrafish, although this might not be evident during embryogenesis.

Implications for myofibrillogenesis models

How do our data impact upon the three current models of myofibrillogenesis outlined in the introduction? The core of all three models is a sequential deposition of the myofibrillar components from Z-line to M-line, with I-Z-I brushes forming first, followed by the integration of thick filaments to complete sarcomeric assembly. Our data support the notion that I-Z-I brushes form first, but that these do not align or become properly spaced in *slo* mutants leaving no well-structured scaffold onto which thick filaments can integrate. Thus, our data suggest a more active role for the assembly and integration of thick filaments in the linking together, alignment and spacing of Z-discs during sarcomere maturation.

Both Sanger's model (Sanger et al., 2002) and the 'Titin' model (Trinick and Tskhovrebova, 1999) of myofibrillogenesis suggest that a well-formed scaffold of I-Z-I brushes is established prior to thick filament integration, with either non-muscle Myosin or Titin fulfilling the role of linking the I-Z-I brushes. In both cases, the lack of assembly and integration of thick filaments should not significantly impact upon the construction of the sarcomeric scaffold. In slo^{u45} mutants, scaffold formation is compromised as I-Z-I brushes do not properly align, are not correctly spaced and probably do not

correctly lace up with adjacent I-Z-I brushes. This suggests either that Hsp90a has unsuspected roles in the assembly of non-muscle Myosin or Titin, or that the models might need some revision. Indeed, Titin immunohistochemistry in *slo*^{u45} mutants suggests that the molecule is not even correctly integrated into the I-Z-I brushes that are present, raising the possibility that sarcomeric Titin integration might lie parallel to, or even downstream of, thick filament assembly and integration. The third model of myofibrillogenesis (Ehler et al., 1999) holds that I-Z-I brushes are loaded with thick filaments at specific cellular locations and subsequently assembled into full sarcomeres. The *slo*^{u45} phenotype is not inconsistent with this idea, but neither does it provide strong support.

The mutants described in this and related papers enhance our understanding of myofibrillogenesis through study of the process in vivo. We are hopeful that further genetic studies of sarcomere formation will refine existing models and help build a more complete picture of myofibrillogenesis.

The study was supported by the BBSRC, Wellcome Trust and EC ZF-Models Integrated Project (http://zf-models.org). Hsp90 work at ICR is supported by the Wellcome Trust (L.H.P.). A.-P.H. was supported by an EC Marie-Curie Fellowship and R.A. by a BBSRC David Phillips Fellowship. T.A.H. received a UCL Bogue Fellowship to visit Stanford University. We thank Mike Hubank and Nipurna Jina (ICH Gene Microarray Centre) for microarray processing; Phil Ingham, Sarah Baxendale, Elizabeth Busch and Derek Stemple for sharing data and information prior to publication; Rodrigo Young and Mark Turmaine for practical assistance; Hans-Georg Frohnhöfer and Carole Wilson and her team for fish care.

Supplementary material

Supplementary material for this article is available at
http://dev.biologists.org/cgi/content/full/135/6/1147/DC1

References

Ali, M. M., Roe, S. M., Vaughan, C. K., Meyer, P., Panaretou, B., Piper, P. W., Prodromou, C. and Pearl, L. H. (2006). Crystal structure of an Hsp90-nucleotide-p23/Sba1 closed chaperone complex. *Nature* **440**, 1013-1017.

Barral, J. M., Bauer, C. C., Ortiz, I. and Epstein, H. F. (1998). Unc-45 mutations in Caenorhabditis elegans implicate a CRO1/She4p-like domain in myosin assembly. *J. Cell Biol.* **143**, 1215-1225.

Barral, J. M., Hutagalung, A. H., Brinker, A., Hartl, F. U. and Epstein, H. F. (2002). Role of the myosin assembly protein UNC-45 as a molecular chaperone for myosin. *Science* **295**, 669-671.

Blagg, B. S. and Kerr, T. D. (2006). Hsp90 inhibitors: small molecules that transform the Hsp90 protein folding machinery into a catalyst for protein degradation. *Med. Res. Rev.* **26**, 310-338.

Chun, M. and Falkenthal, S. (1988). Ifm(2)2 is a myosin heavy chain allele that disrupts myofibrillar assembly only in the indirect flight muscle of Drosophila melanogaster. *J. Cell Biol.* **107**, 2613-2621.

Clark, K. A., McElhinny, A. S., Beckerle, M. C. and Gregorio, C. C. (2002). STRIATED MUSCLE CYTOARCHITECTURE: an intricate web of form and function. *Annu. Rev. Cell Dev. Biol.* **18**, 637-706.

Cooke, R. (2004). The sliding filament model: 1972-2004. *J. Gen. Physiol.* **123**, 643-656.

Dan-Goor, M., Silberstein, L., Kessel, M. and Muhlrad, A. (1990). Localization of epitopes and functional effects of two novel monoclonal antibodies against skeletal muscle myosin. *J. Muscle Res. Cell Motil.* **11**, 216-226.

Ehler, E., Rothen, B. M., Hammerle, S. P., Komiyama, M. and Perriard, J. C. (1999). Myofibrillogenesis in the developing chicken heart: assembly of Z-disk, M-line and the thick filaments. *J. Cell Sci.* **112**, 1529-1539.

Etard, C., Behra, M., Fischer, N., Hutcheson, D., Geisler, R. and Strahle, U. (2007). The UCS factor Steif/Unc-45b interacts with the heat shock protein Hsp90a during myofibrillogenesis. *Dev. Biol.* **308**, 133-143.

Fulton, A. B. and L'Ecuyer, T. (1993). Cotranslational assembly of some cytoskeletal proteins: implications and prospects. *J. Cell Sci.* **105**, 867-871.

Fulton, A. B. and Alftine, C. (1997). Organization of protein and mRNA for titin and other myofibril components during myofibrillogenesis in cultured chicken skeletal muscle. *Cell Struct. Funct.* **22**, 51-58.

Fürst, D. O., Osborn, M., Nave, R. and Weber, K. (1988). The organization of titin filaments in the half-sarcomere revealed by monoclonal antibodies in immunoelectron microscopy: a map of ten nonrepetitive epitopes starting at the Z line extends close to the M line. *J. Cell Biol.* **106**, 1563-1572.

Fürst, D. O., Osborn, M. and Weber, K. (1989). Myogenesis in the mouse embryo: differential onset of expression of myogenic proteins and the involvement of titin in myofibril assembly. *J. Cell Biol.* **109**, 517-527.

Gotthardt, M., Hammer, R. E., Hubner, N., Monti, J., Witt, C. C., McNabb, M., Richardson, J. A., Granzier, H., Labeit, S. and Herz, J. (2003). Conditional expression of mutant M-line titins results in cardiomyopathy with altered sarcomere structure. *J. Biol. Chem.* **278**, 6059-6065.

Granato, M., van Eeden, F. J., Schach, U., Trowe, T., Brand, M., Furutani-Seiki, M., Haffter, P., Hammerschmidt, M., Heisenberg, C. P., Jiang, Y. J. et al. (1996). Genes controlling and mediating locomotion behavior of the zebrafish embryo and larva. *Development* **123**, 399-413.

Gregorio, C. C., Granzier, H., Sorimachi, H. and Labeit, S. (1999). Muscle assembly: a titanic achievement? *Curr. Opin. Cell Biol.* **11**, 18-25.

Hinits, Y. and Hughes, S. M. (2007). Mef2s are required for thick filament formation in nascent muscle fibres. *Development* **134**, 2511-2519.

Holtzer, H., Hijikata, T., Lin, Z. X., Zhang, Z. Q., Holtzer, S., Protasi, F., Franzini-Armstrong, C. and Sweeney, H. L. (1997). Independent assembly of 1.6 microns long bipolar MHC filaments and I-Z-I bodies. *Cell Struct. Funct.* **22**, 83-93.

Krone, P. H., Lele, Z. and Sass, J. B. (1997). Heat shock genes and the heat shock response in zebrafish embryos. *Biochem. Cell Biol.* **75**, 487-497.

LoRusso, S. M., Rhee, D., Sanger, J. M. and Sanger, J. W. (1997). Premyofibrils in spreading adult cardiomyocytes in tissue culture: evidence for reexpression of the embryonic program for myofibrillogenesis in adult cells. *Cell Motil. Cytoskeleton* **37**, 183-198.

Musa, H., Meek, S., Gautel, M., Peddie, D., Smith, A. J. and Peckham, M. (2006). Targeted homozygous deletion of M-band titin in cardiomyocytes prevents sarcomere formation. *J. Cell Sci.* **119**, 4322-4331.

Panaretou, B., Prodromou, C., Roe, S. M., O'Brien, R., Ladbury, J. E., Piper, P. W. and Pearl, L. H. (1998). ATP binding and hydrolysis are essential to the function of the Hsp90 molecular chaperone in vivo. *EMBO J.* **17**, 4829-4836.

Pearl, L. H. and Prodromou, C. (2006). Structure and mechanism of the hsp90 molecular chaperone machinery. *Annu. Rev. Biochem.* **75**, 271-294.

Proisy, N., Sharp, S. Y., Boxall, K., Connelly, S., Roe, S. M., Prodromou, C., Slawin, A. M., Pearl, L. H., Workman, P. and Moody, C. J. (2006). Inhibition of hsp90 with synthetic macrolactones: synthesis and structural and biological evaluation of ring and conformational analogs of radicicol. *Chem. Biol.* **13**, 1203-1215.

Rhee, D., Sanger, J. M. and Sanger, J. W. (1994). The premyofibril: evidence for its role in myofibrillogenesis. *Cell Motil. Cytoskeleton* **28**, 1-24.

Rossi, A. E. and Dirksen, R. T. (2006). Sarcoplasmic reticulum: the dynamic calcium governor of muscle. *Muscle Nerve* **33**, 715-731.

Sanger, J. W., Chowrashi, P., Shaner, N. C., Spalthoff, S., Wang, J., Freeman, N. L. and Sanger, J. M. (2002). Myofibrillogenesis in skeletal muscle cells. *Clin. Orthop. Relat. Res.* **403**, S153-S162.

Schultheiss, T., Lin, Z. X., Lu, M. H., Murray, J., Fischman, D. A., Weber, K., Masaki, T., Imamura, M. and Holtzer, H. (1990). Differential distribution of subsets of myofibrillar proteins in cardiac nonstriated and striated myofibrils. *J. Cell Biol.* **110**, 1159-1172.

Sellers, J. R. (2004). Fifty years of contractility research post sliding filament hypothesis. *J. Muscle Res. Cell Motil.* **25**, 475-482.

Trinick, J. and Tskhovrebova, L. (1999). Titin: a molecular control freak. *Trends Cell Biol.* **9**, 377-380.

Van der Ven, P. F., Ehler, E., Perriard, J. C. and Furst, D. O. (1999). Thick filament assembly occurs after the formation of a cytoskeletal scaffold. *J. Muscle Res. Cell Motil.* **20**, 569-579.

Venolia, L., Ao, W., Kim, S., Kim, C. and Pilgrim, D. (1999). unc-45 gene of Caenorhabditis elegans encodes a muscle-specific tetratricopeptide repeat-containing protein. *Cell Motil. Cytoskeleton* **42**, 163-177.

Zhao, R., Davey, M., Hsu, Y. C., Kaplanek, P., Tong, A., Parsons, A. B., Krogan, N., Cagney, G., Mai, D., Greenblatt, J. et al. (2005). Navigating the chaperone network: an integrative map of physical and genetic interactions mediated by the hsp90 chaperone. *Cell* **120**, 715-727.